Dimers of Glutaredoxin 2 as Mitochondrial Redox Sensors in Selenite-induced Oxidative Stress

Metallomics

Accepted Manuscript

This article can be cited before page numbers have been issued, to do this please use: V. SCALCON, F. Tonolo, A. Folda, A. Bindoli and M. P. Rigobello, *Metallomics*, 2019, DOI: 10.1039/C9MT00090A.

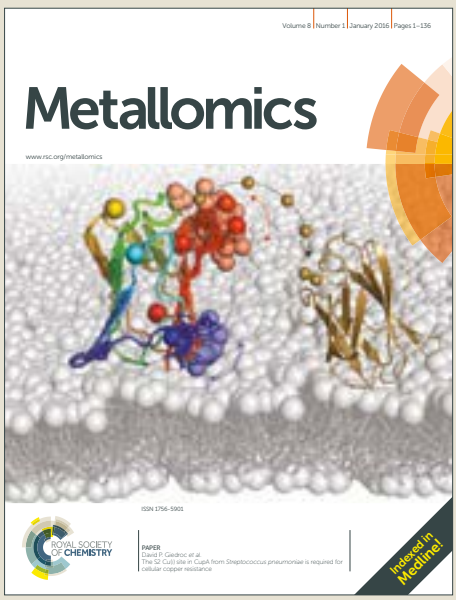

ROYAL SOCIETY OF CHEMISTRY

rsc.li/metallomics

View Article Online
DOI: 10.1039/C9MT00090A

Significance to Metallomics

Iron-sulfur clusters are crucial in mitochondria physiology. The thiol protein glutaredoxin (Grx2), mainly located in the mitochondrial matrix, coordinates an iron-sulfur cluster, forming inactive dimers stabilized by two molecules of glutathione, while the monomeric active form catalyzes protein glutathionylation/de-glutathionylation. Grx2 is connected to the two major systems devoted to thiol redox regulation, as it is reduced by both glutathione and thioredoxin reductase. Grx2 monomerization, determining iron release, drives to apoptotic process. Therefore, the regulation mechanism of Grx2 is of great interest both in mitochondrial iron metabolism and in iron-dependent peroxidation processes.

Metallomics

View Article Online
DOI: 10.1039/C9MT00090A

ARTICLE

Received 00th January 20xx,

Accepted 00th January 20xx

DOI: 10.1039/x0xx00000x

Dimers of Glutaredoxin 2 as Mitochondrial Redox Sensors in Selenite-induced Oxidative Stress

Valeria Scalcon,[a] Federica Tonolo,[a] Alessandra Folda,[a] Alberto Bindoli [a,b] and Maria Pia Rigobello[a*]

Glutaredoxin 2 (Grx2) has been previously shown to link thioredoxin and glutathione systems by receiving reducing equivalents by both thioredoxin reductase and glutathione. Grx2 catalyzes protein glutathionylation/de-glutathionylation and can coordinate an iron-sulfur cluster, forming inactive dimers stabilized by two molecules of glutathione. This protein is mainly located in the mitochondrial matrix, though other isoforms have been found in the cytosolic and nuclear cell compartments. In the present study, we have analyzed the monomeric and dimeric states of Grx2 under different redox conditions in HeLa cells, and sodium selenite was utilized as the principal oxidizing agent. After selenite treatment, an increased glutathione oxidation was associated to Grx2 monomerization and activation, specifically in the mitochondrial compartment. Interestingly, in mitochondria, a large decline of thioredoxin reductase activity was also observed concomitantly to Grx2 activity stimulation. In addition, Grx2 monomerization led to an increase free iron ions concentration in the mitochondrial matrix, induction of lipid peroxidation and decrease of the mitochondrial membrane potential, indicating that the disassembly of Grx2 dimer involved the release of the iron-sulfur cluster in the mitochondrial matrix. Moreover, sodium selenite-triggered lipid and protein oxidation was partially prevented by deferiprone, an iron chelator with mitochondriotropic properties, suggesting a role of the iron-sulfur cluster release in the observed impairment of mitochondrial functions. Thus, by sensing the overall cellular redox conditions, mitochondrial Grx2 dimers become active monomers upon oxidative stress induced by sodium selenite with the consequent release of the iron-sulfur cluster, leading to activation of the intrinsic apoptotic pathway.

Introduction

Thioredoxin and glutathione systems, active both in the cytosol and mitochondria, control cellular thiol redox homeostasis.[1-3] In addition to several other functions, essentially characterized by a thiol-dependent reducing action, both systems finely tune the concentration of hydrogen peroxide (H_2O_2) through peroxiredoxins and glutathione peroxidases.[3] The two small proteins thioredoxin (Trx) and glutaredoxin (Grx), belonging to the thiol-disulfide oxidoreductase family by sharing a common active-site motif Cys-X-X-Cys,[4] play a pivotal role in their respective systems. Trx and Grx receive electrons from thioredoxin reductase (TrxR) and reduced glutathione (GSH), respectively. NADPH is the common reducing agent acting as a substrate for TrxR, and also maintaining glutathione reduced through the action of glutathione reductase.[1] Of note, Grx has the unique ability to reduce the mixed disulfides occurring between protein thiols and glutathione (deglutathionylation) or, conversely, to catalyze their formation (glutathionylation).[5] This is at variance with Trx which acts only as a general disulfide reducing factor.[6] Both proteins are present in mitochondria with specific isoforms, thioredoxin 2 (Trx2), glutaredoxin 2 (Grx2) and glutaredoxin 5 (Grx5). Grx5 is a monothiol glutaredoxin necessary for the maintenance of cellular iron homeostasis and for iron-sulfur cluster biosynthesis but completely inactive as a redox enzyme.[7] Conversely, Grx2 plays a critical role in the cell defense against oxidative stress and in the regulation of cell death as shown by the increased sensitivity toward doxorubicin and phenyl arsine oxide of Grx2 knock-down HeLa cells obtained by RNA interference.[8] In cells, Grx2 protein concentration is significantly lower than that of the cytosolic isoform Grx1.[9] Unlike the cytosolic Grx1, which at the active site contains the conserved Cys-Pro-Tyr-Cys motif, Grx2 holds the sequence Cys-Ser-Tyr-Cys that confers to the protein a high affinity toward glutathionylated proteins.[10] In addition, this sequence is crucial for the coordination of an iron-sulfur cluster [2Fe-2S] [11, 12] and for its reduction by TrxR, a reaction that becomes significant when the level of GSSG increases.[10, 13]

[a] Dipartimento di Scienze Biomediche, Università degli Studi di Padova, Via Ugo Bassi 58/b, 35131 Padova, Italy.
[b] Istituto di Neuroscienze (CNR) Sezione di Padova, c/o Dipartimento di Scienze Biomediche, Viale G. Colombo 3, 35131 Padova, Italy.
* Corresponding author. e-mail: mariapia.rigobello@unipd.it
Electronic Supplementary Information (ESI) available. See
DOI: 10.1039/x0xx00000x

This latter property further reinforces the key role played by Grx2 in the mitochondrial rescuing of an altered redox balance.[10] In fact, the feature that Grx2 might accept electrons not only by GSH but also from TrxR2, makes it quite critical when mitochondria are subjected to oxidative stress leading to a decrease of the [GSH]/[GSSG] ratio that diminishes the rate of reduction of Grx2 by GSH.[10] Therefore, the alternative reduction pathway of Grx2 via TrxR2 constitutes an efficient backup system for restoring proper redox conditions. Considering the numerous targets of glutathionylation in mitochondria leading to modulation of enzymatic activities, [14-16] Grx2 plays a central role in processes such as mitochondrial redox signaling and apoptosis regulation.[10, 17, 18] In fact, in primary cardiomyocytes the lack of Grx2 alters mitochondrial ultrastructure and energetics, a condition which is not restored by N-acetyl cysteine.[19] Conversely, overexpression of Grx2 in HeLa cells decreases apoptosis induced by 2-deoxy-D-glucose or doxorubicin and observed as prevention of cytochrome c (Cyt c) release and caspase activation.[20]

The mechanism by which the [2Fe-2S] is tethered to Grx2 has been investigated on the human recombinant purified protein by Lillig and colleagues[11, 12] and was ascribed to the coordination of the two iron atoms at the opposite sites of the cluster by the N-terminal active site cysteines (Cys37) of each Grx2 monomer. It has been found that the [2Fe-2S]-bridged dimer is enzymatically inactive, but degradation of the cluster and monomerization of Grx2 activates the protein.[11] The [2Fe-2S] $(Grx2)_2$ complex is further stabilized by two non-covalently bound reduced glutathione molecules that bind both the iron atoms of the cluster with their Cys residues and also the two Grx2 monomers non covalently via hydrogen bonds and Van-der-Waals interactions.[11, 12] Interestingly, bound glutathione is in equilibrium with free glutathione.[11, 12] Conditions of oxidative stress leading to an alteration of the redox state of glutathione can disassemble the cluster forming the enzymatically active monomers.[12] Johansson *et al.*[21] obtained the crystal structure of Grx2 holo dimer and confirmed the involvement of the Cys37 of Grx2 for cluster coordination and the requirement of reduced glutathione for the [2Fe-2S] $(Grx2)_2$ stabilization. Therefore, Grx2 can be kept inactive by a high GSH/GSSG ratio that promotes the formation of a 2Fe-2S-bridged dimer in which the active site cysteine are involved.[21] *In vivo*, Grx2 could get activated under oxidative stress when the GSH/GSSG ratio decreases.[11]

In the present paper, the response of Grx2 to oxidative stress has been investigated. In particular, the effects of sodium selenite (Sel), a well-known oxidizing agent for GSH and protein thiols were examined in HeLa cells with particular reference to the monomer/dimer conditions and activity of Grx2. Moreover, the effects on mitochondria attributable to Grx2 monomerization and release of the [2Fe-2S] cluster have been investigated. Finally, the alterations of the overall redox conditions were examined and correlated to cell viability and cancer cell death.

Experimental

Materials

4-acetamido-4'-((iodoacetyl) amino) stilbene-2,2-disulfonic acid (AIS) was purchased form Invitrogen (Carlsbad, CA, USA), primary antibody anti human Grx2 from IMCO Corporation Ltd (Stockholm, Sweden), anti GSH from Virogen (Watertown, MA, USA), anti β-actin from AbFrontier (Seoul, Republic of Korea), anti GPx4 (EPNCIR144) from Abcam (Cambridge, UK) and the primary antibodies anti TOM20 (FL-145), anti TrxR2 (D-12), anti Cyt c (7H8.C12) and anti pro-caspase 3 (H-277) from Santa Cruz Biotechnology (Dallas, TX, USA). Human recombinant Grx2 was kindly provided by Professor Aristi Fernandes (Karolinska Institutet, Stockholm, Sweden). The probes C11-BODIPY and TMRM were purchased from ThermoFisher (Waltham, MA, USA). All other reagents were purchased from Sigma-Aldrich (St. Louis, MO, USA).

Cell culture

Cervix carcinoma HeLa cells were grown in adhesion using high-glucose Dulbecco's Modified Eagle's Medium (DMEM) with glutaMAX containing 10% fetal calf serum and supplemented with Pen-Strep (Thermo Fisher Scientific, Waltham, MA, USA) at 37°C in 5% carbon dioxide atmosphere.

MTT assay

Cell viability was determined with the 3-[4,5-dimethylthiazol-2-yl]-2,5-diphenyltetrazolium bromide (MTT) reduction assay. HeLa cells (5×10^3) were pre-treated with 0.1 mM deferiprone (DEF, 3-hydroxy-1,2-dimethyl-4(1H)-pyridone) for 6 h and then with increasing concentrations of Sel (2.5-15 μM) for 18 h. At the end of incubation, cells were treated for 3 h at 37 °C with 0.5 mg/mL MTT dissolved in phosphate-buffered saline (PBS). Afterward, 100 μL of stop solution (90% isopropanol/10% dimethyl sulfoxide) were added to each well. After 15 min, the absorbance at 595 and 690 nm was estimated using an Infinite® M200 PRO plate reader (Tecan, Männedorf, CH).

Estimation of total thiol groups

Total thiol groups of HeLa cells (4.5×10^5) treated with increasing concentrations of Sel (5-15 μM) for 18 h, or with Sel at the fixed concentration of 15 μM for 18 h with or without pretreatment with 0.1 mM DEF for 6 h, were measured with the Ellman's assay.[22] At the end of incubation, cells were washed with PBS and then 1 mL of ice-cold 0.2 M Tris-HCl buffer (pH 8.1), containing 7.2 M guanidine was added. The titration of free thiols after addition of 30 mM 5,5'-dithiobis(2-nitrobenzoic acid) (DTNB) was monitored spectrophotometrically at 412 nm.

Determination of glutathione concentration and redox state in cell lysates

HeLa cells (4.5×10^5) were incubated for 18 h with increasing concentrations of Sel (5-20 μM). Then, cells were washed with cold PBS, and directly deproteinized with 6% *meta*-phosphoric acid. After 20 min at 4°C cells were scraped and centrifuged at 15800g for 10 min at 4°C. Supernatants were neutralized with 15% Na_3PO_4 and utilized for total glutathione estimation.[23]Aliquots of the samples were incubated with 0.2

View Article Online
DOI: 10.1039/C9MT00090A

mM NADPH and 0.4 units of glutathione reductase from baker's yeast (Sigma-Aldrich, St. Louis, MO, USA) in 0.2 M Na-K-Pi buffer (pH 7.4) added of 5 mM EDTA. The reaction was started by the addition of 0.25 mM DTNB and the absorbance was monitored spectrophotometrically at 412 nm for about 10 min. The nanomoles of total glutathione were calculated using a standard curve of glutathione. For measurement of oxidized glutathione, sample aliquots were treated with 2% 2-vinylpyridine for 40 min before performing the assay.[24] For protein estimation, cell pellets were washed with 1 mL of ice-cold acetone, centrifuged at 11000g, dried, then dissolved in 62.5 mM Tris-HCl buffer (pH 8.1) containing 1% SDS and analyzed by the Lowry assay.[25]

Preparation of cytosol and mitochondria enriched cell fractions after treatment with Sel

To obtain cytosolic and mitochondrial fractions, HeLa cells (3 x 10^7) were grown in 75 cm^2 flasks and then treated with 15 µM Sel for 3, 6, 12 or 18 h. After incubation, cells were processed to obtain mitochondria and cytosol enriched fractions essentially following the protocol of Clayton and Shadel.[26] Briefly, cells were collected, washed with PBS and subjected to hypo-osmotic treatment with 2 mL of ice-cold 10 mM NaCl, 1.5 mM $MgCl_2$, 10 mM Tris-HCl buffer (pH 7.5) for 5 min and gently homogenized using a Dounce tissue grinder. After this treatment, 1.4 mL of 525 mM mannitol, 175 mM sucrose, 2.5 mM EDTA and 12.5 mM Tris-HCl buffer (pH 7.5) were rapidly added. Then, the homogenate was diluted to a final volume of 5 mL with 210 mM mannitol, 70 mM sucrose, 1 mM EDTA and 5 mM Tris-HCl buffer (pH 7.5) and subjected to differential centrifugation. The first step was carried out at 1300g for 5 min at 4°C to discard nuclei and non-disrupted cells. The mitochondrial fraction was pulled down from the supernatant at 15800g for 15 min at 4°C and washed twice. The crude soluble supernatant obtained from the mitochondrial isolation step was further centrifuged at 105000g for 15 min to obtain the cytosolic fraction. Afterwards, mitochondrial samples were lysed using a modified RIPA buffer formed by 150 mM NaCl, 50 mM Tris-HCl (pH 7.4), 1 mM EDTA, 0.1% SDS, 0.5% DOC and 1 mM NaF. Finally, both cell fractions were subjected to protein determination with the Lowry assay.[25] To analyze the amount of Grx2, TrxR2 and TOM20 in the mitochondrial fraction, aliquots of lysed mitochondria (20 µg proteins) were subjected to 12% SDS-PAGE in reducing conditions. After gel electrophoresis, the relative amount of proteins was assessed by Western blot analysis.

Estimation of Grx, TrxR1 and TrxR2 activities

The standard assay for Grx activity is based on the procedure developed by Mieyal *et al*.[27] and modified by Raghavachari and Lou.[28] The reaction mixture contains 0.2 mM NADPH, 0.5 mM GSH, 0.2 M Na-K-Pi buffer (pH 7.4), 0.4 units of glutathione reductase, 5 mM EDTA and an aliquot of purified Grx2 (or 50 µg of cell fractions or mouse liver mitochondria) in a total volume of 1 mL. Reaction was carried out at 30°C with 2 mM hydroxyethyl disulfide (HEDS). The decrease of NADPH absorbance at 340 nm was monitored for 5 min. To determine glutaredoxin activity, the slope of the linear portion of the time course at 340 nm was utilized. Both cytosolic and mitochondrial HeLa cell fractions (50 µg of proteins) were tested also for TrxR activity in 0.2 M Na-K-Pi buffer (pH 7.4) containing 5 mM EDTA and 20 mM DTNB. After 2 min, 0.25 mM NADPH was added and the reaction was followed at 412 nm, at 25°C.

Isolation of mouse liver mitochondria and treatment with reducing agents

Three months old male C57bl/6 mice were euthanized through cervical dislocation. Liver was quickly removed, rinsed, and mitochondria were isolated through differential centrifugations as previously described.[29] Protein content was determined via the Bradford assay.[30] Aliquots of mitochondria (200 µg proteins) were lysed in RIPA buffer and treated with either 1 mM GSH or 10 mM sodium dithionite for 30 min at room temperature.[31] Afterwards, Grx2 specific activity was assessed as described in the previous subparagraph. Animal care and relative experimentation were performed in accordance with European and Italian laws (D.L. 26/2014) concerning animal used for scientific purposes. All the protocols were approved by the Ethical Committee of University of Padova and all the animals are from an internal animal house authorized by the Ministry of Health (N. 102/2004-A).

Determination of Grx2 monomerization in whole cell lysates or isolated mitochondria

For the determination of Grx2 monomerization, the procedure of Stanley *et al.*[32] with modifications was followed. After incubation with 15 µM Sel for 18 h, HeLa cells were collected and washed with cold PBS. Then, cells were either subjected to cell fractionation as reported above or treated with 1 mL of 10% trichloracetic acid (TCA) at 4°C for 30 min, and then centrifuged for 15 min at 15800g at 4°C. Pellets washed with 1 mL of ice-cold acetone, were then centrifuged at 10000g for 10 min at room temperature. Afterwards, TCA treated cell samples or isolated mitochondria were dissolved in 670 mM Tris-HCl buffer (pH 7.5) containing 2% SDS and 10 mM AIS. Derivatization lasted for 20 min at room temperature, followed by further 45 min at 37°C. Samples were subjected to protein determination with the Lowry assay [25] and aliquots (20 µg of proteins) were loaded, without reducing agents, onto a 12% Bis-Tris Gel NU-PAGE Invitrogen (Carlsbad, CA, USA). Finally, Grx2 monomer and dimer were revealed in Western blot using an anti Grx2 antibody.

Quantification of the labile iron pool in mitochondria isolated from HeLa cells treated with Sel

HeLa cells (3 x 10^7) were grown in 75 cm^2 flasks and then treated with 15 µM Sel for 18 h. After incubation, cells were processed to obtain mitochondria and cytosol enriched fractions essentially following the protocol of Clayton and Shadel already described above.[26] Soon after isolation, mitochondria were treated with 600 µL of 6% *meta*-phosphoric acid for 20 min at 4°C in order to obtain the acid-

View Article Online
DOI: 10.1039/C9MT00090A

labile iron pool. At the end of incubation, samples were centrifuged at 15800g for 10 min at 4°C and the pellet was subjected to protein determination. Both the pellet and the supernatant were mineralized and the total amount of iron was estimated by atomic absorption spectroscopy. Briefly, samples were subjected to five cycles of freezing-thawing at -20/+32°C of 20 min, mineralized in 200 µL of highly purified nitric acid (Fe: ≤0.01 mg/kg) plus 200 µL H_2O_2 and then transferred into a microwave Teflon vessel before being subjected to the standard procedure using a speed wave MWS-3 Berghof instrument (Berghof, Eningen, Germany). Fe content of each sample was determined using a Varian AA Duo graphite furnace atomic absorption spectrometer (Varian, Palo Alto, CA, USA) at the wavelength of 248.3 nm.

Determination of lipid peroxidation in HeLa cells

Lipid peroxidation was analyzed in cells by flow cytometry and measurement of malondialdehyde (MDA) production. HeLa cells (4.5 x 10^5) were treated for 18 h in the presence of 15 µM Sel with or without pretreatment with 0.1 mM DEF or with 0.1 mM butylated hydroxytoluene (BHT). For the FACS estimation of lipid peroxidation, at the end of incubation, cells were loaded with 2 µM C11-BODIPY probe diluted in PBS/10 mM glucose, for 30 min at 37°C in the dark. Then, cells were trypsinized and resuspended in PBS/10 mM glucose at a concentration of 2.5 x 10^5/mL. Lipid peroxidation was measured on the FITC-1 channel with a FACSCanto™ II flow cytometer (Becton-Dickinson, Franklin Lakes, NJ, USA) using a blue laser at 488 nm. For MDA production, cells treated with 15 µM Sel with or without pre-treatment with the iron-chelator (0.1 mM DEF), were washed with PBS and treated with 1 mL of 0.1 N H_2SO_4 and 150 µL of 10% phosphotungstic acid (PTA) for 10 minutes at room temperature. Then, cells were centrifuged at 15800g for 10 min at 4°C. Discarded the supernatants, the pellets were resuspended in 1 mL of 0.1 N H_2SO_4 and 150 µL of PTA and again centrifuged as described above. Afterwards, the pellets were dissolved with 350 µL of a medium composed by 0.25% NONIDET P-40, 0.01% BHT, 0.17% thiobarbituric acid and incubated at 95°C for 60 min. At the end, samples were ice-cooled for 5 min and centrifuged at 15800g for 10 min. Supernatants were treated with 400 µL of *n*-butanol, vigorously mixed and centrifuged at 15800g for 15 min. The fluorescence of the upper phase was estimated (Ex: 530 nm; Em: 590 nm) using a Tecan Infinite® M200 PRO plate reader (Tecan, Männedorf, CH). For protein determination,[25] the pellets were washed with 500 µL of acetone/HCl solution (98:2) for 10 min at 4°C, centrifuged at 15800g for 10 min at 4°C and dissolved in 75 µL of RIPA buffer.

Measurement of mitochondrial membrane potential in HeLa cells

Mitochondrial membrane potential of HeLa cells was analyzed by flow cytometry. HeLa (4.5 x 10^5 cells) were treated for 18 h with 15 µM Sel. Cells were then collected, resuspended in PBS/10 mM glucose and loaded with 25 nM tetramethylrhodamine methyl ester (TMRM) at 37 °C in the dark, for 15 min. Membrane potential was estimated with a FACSCanto™ II flow cytometer using a blue laser at 488 nm.

Estimation of cytochrome c release and caspase 3 activation

Cyt c release and caspase 3 activation were detected using the Western blot technique. After 18 h of incubation in the presence of 15 µM Sel, HeLa cells (4.5 x 10^5) were harvested, washed with PBS, treated with a hypotonic lysis buffer (20 mM Hepes-Tris buffer (pH 7.5), 10 mM KCl, 1.5 mM $MgCl_2$, 1 mM EDTA and 1 mM EGTA) and added with an antiprotease cocktail (Complete, Roche, Mannheim, DE) for 15 min. Then, the suspension was centrifuged at 12500g for 10 min at 4°C. The supernatant, added with 0.5 mM EGTA and 2.5 mM phenylmethanesulfonyl fluoride was centrifuged for 30 min at 105000g at 4°C. Aliquots of 10 mg protein of the supernatants and of the pellets were subjected to SDS-PAGE (15%) followed by Western blot using a cytochrome c monoclonal antibody and a pro-caspase 3 polyclonal antibody. β-actin content was determined as a loading control for the cytosolic compartment and TOM20 for the mitochondrial one. A peroxidase-conjugated secondary antibody and chemiluminescence were used to detect the immunoreactive bands.[33]

Statistical analysis

All the experimental data reported are the mean, with their respective SD, of at least three experiments. Comparisons between two groups were performed using non paired two-tailed Student's t-test and analysis of variance was performed by multiple comparison test with Tukey-Kramer method utilizing INSTAT 3.3 (GraphPad) software. A value of $p<0.05$ was considered significant.

Results

Effect of Sel treatment on cellular thiol redox state

HeLa cells, treated with increasing concentrations of Sel, show a marked decrease of total thiol groups and glutathione (Fig. 1). In particular, total glutathione decrease is accompanied by a decrease of the ratio GSH/GSSG.

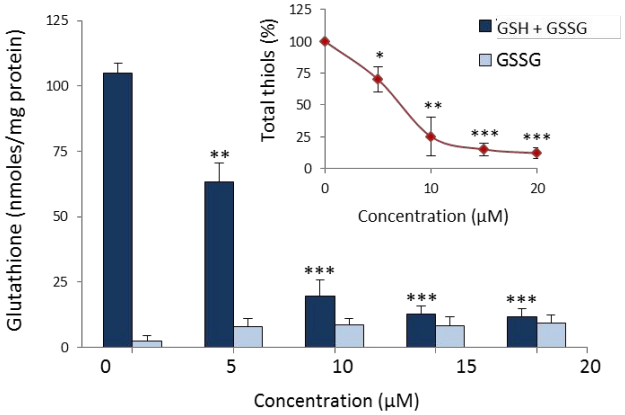

Figure 1. Effect of Sel treatment on cellular thiol redox state. HeLa cells (4.5 x 10^5) were treated for 18 h with increasing concentrations of Sel (5-20 µM). Then, cells were processed and total (GSH + GSSG) and oxidized (GSSG) glutathione levels were assessed as reported in

View Article Online
DOI: 10.1039/C9MT00090A

Experimental. Inset: measurement of total free thiol concentration of HeLa cells, treated in the same conditions, as percentage with respect to the control. (*p<0.05, **p<0.01, ***p<0.001)

This result, in line with previous observations,[34, 35] indicates that glutathione might either be released from cells or can be found covalently bound to proteins as a mixed disulfide. In our conditions, 15 µM Sel is required for the almost complete oxidation of glutathione and thus it has been chosen for the subsequent experimentation.

Sel leads to Grx2 monomerization in cells

The ability to form dimers linked together by an iron-sulfur cluster is a specific feature of Grx2.[11] In order to estimate the transition from dimeric to monomeric form, HeLa cells were treated with Sel, then lysed and subjected to non-reducing gel electrophoresis and Western blot. As apparent in Fig. 2 A and B, both in whole cell lysates and in cell mitochondrial fractions, the dimeric form is neatly prevailing over the monomeric one in basal conditions, while, after treatment with Sel, the monomer largely increases. Indeed, treatment for 18 hours with 15 µM Sel results in the transition to Grx2 monomer especially in the mitochondrial cell compartment (Fig. 2 B and B'). Interestingly, three bands can be observed for the dimeric form especially when assessed in isolated mitochondria. This result can suggest the differential presence of the two glutathione moieties involved in the stabilization of the dimer. In particular, the upper band corresponds to the [2Fe-2S] $(Grx2)_2$ cluster with both GSH coordinated, whereas the other two bands may be ascribed to the cluster with one or without GSH. In support of this finding, the same Western blot membrane was also incubated with an antibody raised against glutathione. As expected, GSH was detected in correspondence to the upper band of Grx2 dimer while no staining was shown for the monomer or in cells treated with Sel (Fig. S 1 of the electronic supplementary information). This indicates that the oxidation of glutathione induced by Sel can be perceived by the holo dimer through the oxidation and detachment of the GSH molecules involved in the stabilization of the complex. Interestingly, Grx2 protein level in mitochondria is not decreased by treatment of cells with Sel (Fig. 2 C and C') indicating that the increase of monomeric Grx2 is due to the disassembly of the dimer.

In addition to Sel, also other conditions leading to oxidative stress such as depletion of glutathione by treatment with buthionine sulfoximine (BSO), an inhibitor of GSH synthesis, in combination with auranofin (AF), that inhibits TrxR activity, trigger the monomerization of Grx2 (Fig. S 2 of the electronic supplementary information).

Monomeric Grx2 is active as a disulfide reductase in the mitochondrial compartment

In order to estimate the effects of oxidizing conditions on Grx2 activity, the specific enzymatic activity of glutaredoxin was measured in both the cytosolic and the mitochondrial cell compartments over time, ranging from 3 to 18 hours after administration of Sel to cells. Since in the cytosol both Grx1 and Grx2 are present and considering that both isoforms are active in the enzymatic activity assay, only the overall glutaredoxin activity can be measured. In the mitochondrial matrix, in addition to Grx2, only the monothiol Grx5, inactive as disulfide reductase, is present and thus the enzymatic activity assessed for glutaredoxin basically corresponds to Grx2. Indeed, yeast Grx5 was reported to be inactive in the thiol transferase assay using HEDS as substrate.[36] Of note, in the mitochondrial intermembrane space Grx1 has also been found.[37] Therefore, the mitochondrial glutaredoxin activity measured is the sum between Grx2 present in the matrix and Grx1 located in the IMS. However, Grx1 concentration is at least 10 fold less than Grx2 (0.1 µM for Grx1 in the IMS versus 1 µM for Grx2 in the matrix).[38] Hence, the activity measured in the assay corresponds principally, even though not solely, to Grx2. As reported in Fig. 3 A and Fig. S 3 of the electronic supplementary information, total Grx activity in the cytosolic cell fraction does not significantly decrease upon Sel administration. A quite interesting result was found in the

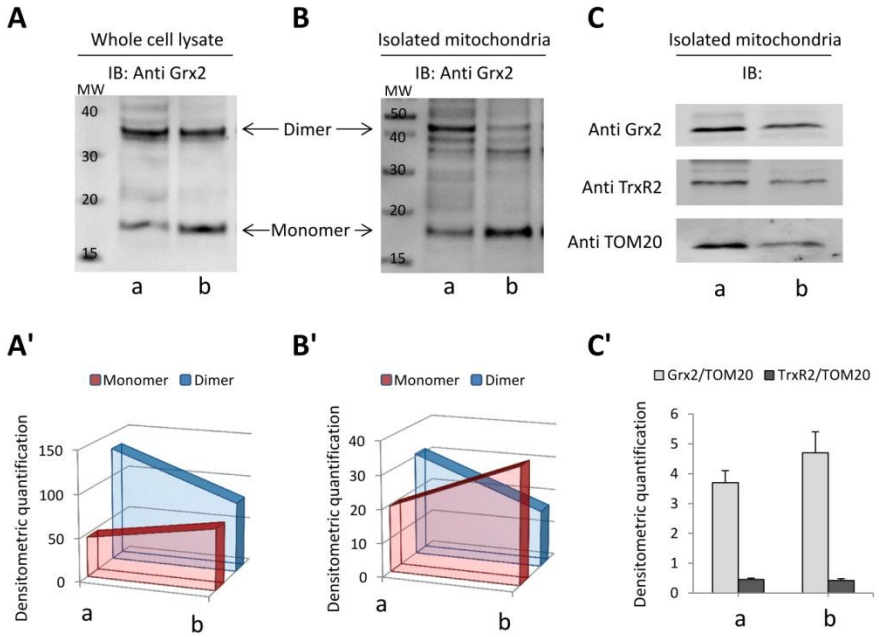

Figure 2. Grx2 monomerization and quantification in Sel treated cells. HeLa cells were treated for 18 h with 15 µM Sel. To analyze the monomerization of Grx2, whole cell samples (**A**) or mitochondrial cell fractions (**B**), derivatized with 10 mM AIS, were subjected to NU-PAGE in non-reducing conditions and WB analysis. **a**: cnt; **b**: 15 µM Sel. (**C**) HeLa cells (3×10^7) were treated for 18 h with 15 µM Sel and then subjected to cell sub-fractionation in order to obtain the mitochondrial enriched fraction. The isolated mitochondria were then probed for Grx2, TrxR2 and TOM20 protein levels. (**a**): Cnt; (**b**): 15 µM Sel. (**A'**), (**B'**) and (**C'**) report the densitometric analysis of data shown in panel (**A**), (**B**) and (**C**), respectively, performed with NineAlliance software.

View Article Online
DOI: 10.1039/C9MT00090A

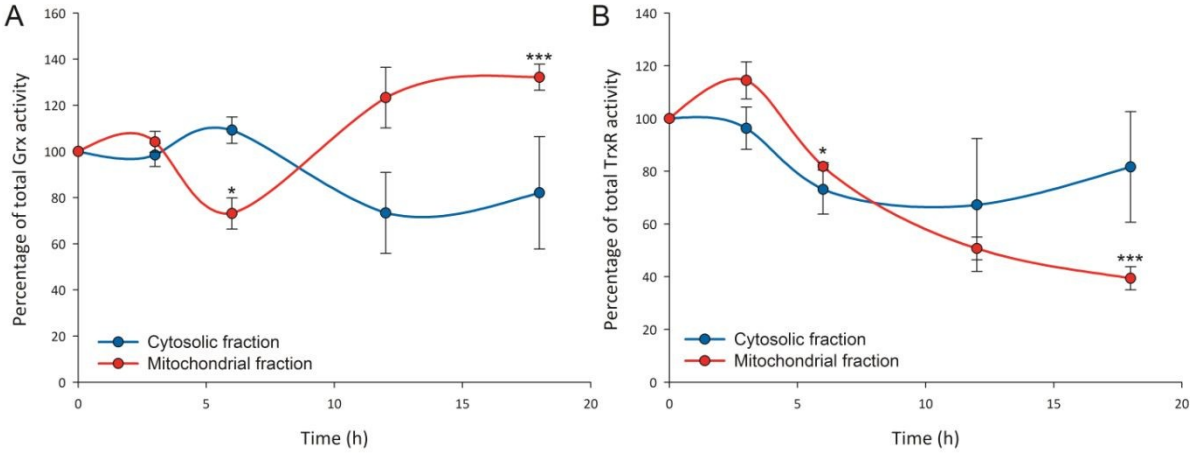

Figure 3. Time-scale analysis of total glutaredoxin (A) and thioredoxin reductase (B) activities in the cytosolic and mitochondrial compartments of Sel treated cells. HeLa cells (3 x 10^7) were treated for 3, 6, 12 and 18 h with 15 μM Sel and then subjected to cell sub-fractionation in order to obtain the cytosolic and mitochondrial fractions. The two cell fractions were then probed for the various enzymatic activities. (*p<0.05, ***p<0.001)

mitochondrial fraction where Grx2 activity exhibits a biphasic effect (Fig. 3 A). In particular, Grx2 activity after an initial decrease in the first 6 hours following Sel addition, increases of about 30% at 18 hours of incubation, in accordance to the observed induction of protein monomerization in that specific time-frame (Fig. 2 B and B').

Considering that total glutathione concentration largely decreases upon HeLa cell treatment with Sel and that the residual glutathione amount is mainly oxidized (Fig. 1), we investigated whether TrxR2 could be the electron supplier that promotes Grx2 activity. In fact, Grx2 was previously reported to be able to receive reducing equivalents also from TrxR2 acting as a backup mechanism for the glutathione system.[10] As shown in Fig. 3 B, in the cytosol, TrxR1 activity initially slightly decreases but eventually returns to the initial values at 18 hours. On the contrary, in mitochondria, TrxR2 activity is stimulated at first but then drops at longer incubation times (Fig. 3 B and S 3). This finding suggests that Grx2 monomerization takes place in stress conditions where both the major thiol redox regulating systems are impaired. Therefore, Grx2 activity seems to be particularly important in the mitochondrial cell compartment with respect to the cytosolic one. Of note, treatment of human recombinant Grx2 with Sel up to 20 μM did not affect its enzymatic activity (data not shown). This result rules out a direct effect of Sel on the protein itself and highlights a probable involvement of glutathione and the iron-sulfur cluster in the observed Grx2 activity.

Mitochondrial Grx2 monomerization as consequence of oxidative stimuli

In order to see whether protein monomerization upon induction of different redox stimuli is due to the ability of the dimer to sense redox alterations in the environment, Grx2 activity was measured in isolated mouse liver mitochondria lysed with RIPA buffer as described in Experimental. Interestingly, treatment with 1 mM GSH decreases Grx2 activity with respect to untreated mitochondria (Fig. 4) probably by stabilization of the protein in its dimeric form. Conversely, sodium dithionite (DT) induces Grx2 activity possibly by donating an electron to molecular oxygen to form superoxide anion acting as one electron oxidant of iron in the iron-sulfur cluster, as previously suggested.[31] Therefore, these results support the idea of a redox-mediated protein modulation as an oxidizing environment is able to trigger Grx2 monomerization and activation.

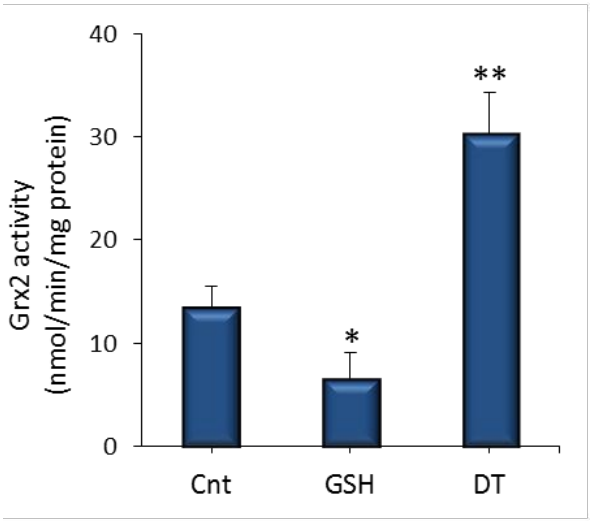

Figure 4. Determination of Grx2 activity on isolated mouse liver mitochondria. Mouse liver mitochondria were isolated and lysed as described in the Experimental section. Grx2 activity was measured in control conditions or after 30 min incubation with 1 mM glutathione (GSH) to mimic a reducing condition or with 10 mM sodium dithionite (DT). (*p<0.05, **p<0.01)

Grx2 dimer dissociation determines iron release

Since Grx2 monomerization involves the dissociation of the dimer and the disassembly from the iron-sulfur cluster, we

View Article Online
DOI: 10.1039/C9MT00090A

decided to analyze the effect of redox imbalance on iron release by cluster disruption in the mitochondrial matrix. Therefore, the concentration of mitochondrial free iron pool in HeLa cells treated with 15 µM Sel for 18 h were compared to control cells. Briefly, the isolated mitochondrial fraction of cells incubated with Sel (15 µM for 18 h) was treated with *meta*-phosphoric acid in order to separate the acid-labile iron from the protein-bound pool. Then, iron was quantified by using atomic absorption spectroscopy as described in Experimental. As reported in Table 1 the concentration of free iron, normalized for the protein content in Sel treated sample, is twice as much as the control, supporting our hypothesis of a release of iron deriving from the disruption of the iron-sulfur clusters of Grx2 following its monomerization. The increase of mitochondrial labile iron in Sel-treated cell is statistically significant with respect to the control with $p<0.01$.

Table 1. Amount of labile iron in mitochondria of HeLa cells upon Sel treatment (mean ± SD of 4 replicates).

	µg Fe/mg protein
Cnt	9.5 ± 4.9
Sel 15 µM	21.0 ± 7.1

In addition, the non acid-labile iron pool corresponding mainly to the protein-bound and heme iron, was also estimated utilizing the same protocol (Fig. S 4 of the electronic supplementary information). The increase of the acid-labile fraction in mitochondria of Sel-treated cells, suggests an impairment of the iron-handling capacity and possible disruption of the complex iron-processing machine leading to the observed mitochondrial iron overload.

The increased mitochondrial iron content drives to apoptosis

The mitochondrial increase of free-iron can trigger lipid peroxidation[39] and lead to cell death.[18, 40] Thus, we decided to determine whether Sel-mediated iron release in mitochondria could stimulate lipoperoxidation and activate apoptosis. We utilized the C11-BODIPY fluorescent dye and analyzed cell fluorescence by flow cytometry. As expected, HeLa cells treated with Sel for 18 h displayed a significant increase of fluorescence indicating the occurrence of lipid peroxidation (Fig. 5 A). The induction of lipid peroxidation in cells triggered by Sel administration was partially prevented by the addition of the lipophilic antioxidant butylated hydroxytoluene (BHT) (Fig. S 5 of the electronic supplementary information) indicating that the increase in fluorescence intensity observed was specifically due to the lipoperoxidation of cells. We further analyzed the status of the mitochondrial membrane potential which is known to be affected by cardiolipin oxidation.[41] As shown in Fig. 5 B the mitochondrial membrane potential is largely decreased in cells treated with Sel, with respect to the control, indicating the impairment of mitochondrial functions. The decrease of the mitochondrial membrane potential was also associated to the release of pro-apoptotic factors from mitochondria to the cytosol such as Cyt c. Indeed, as reported

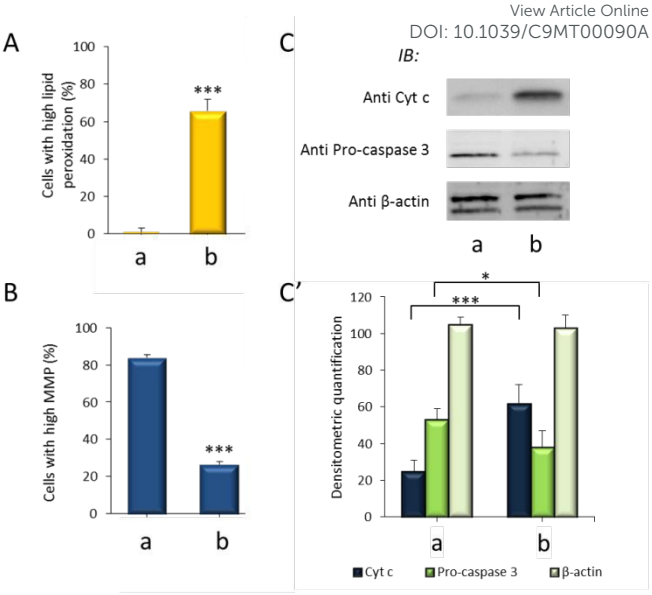

Figure 5. Analysis of the apoptotic pathway activation in Sel treated cells. HeLa cells were treated for 18 h with 15 µM Sel. (**A**) FACS analysis of lipid peroxidation utilizing the C11-BODIPY dye. The graph shows the percentage of cells with a high level of lipid peroxidation. (**B**) FACS analysis of the mitochondrial membrane potential (ΔΨm) of HeLa cells by means of the TMRM probe. The percentage of cells with high ΔΨm is reported. (**C**) Cyt c release and cleavage of the pro-caspase 3 in the cell cytosolic compartment in Sel treated or control cells. β-actin is reported as a loading control. (**C'**) Densitometric analysis of the Western blot bands shown in **C**. (**a**) Cnt; (**b**) 15 µM Sel. For each experiment the mean ± SD of three replicates is shown (*p<0.05; ***p<0.001).

in Fig. 5 C and C' the amount of Cyt c in the cytoplasm of cells treated with Sel increases. Accordingly, we also found that the caspase pathway was activated. Fig. 5 C and C' clearly show that the band corresponding to the inactive form of caspase 3 (pro-caspase 3) decreases in cells treated with Sel, indicating that the protein has been cleaved and activated. The purity of the obtained cytosolic fraction and the corresponding decrease of the amount of Cyt c in the mitochondrial fraction have also been checked (Fig. S 6 of the electronic supplementary information). Altogether these results point out that the release of free iron ions in mitochondria following cell incubation with Sel, by oxidizing mitochondrial membrane lipids, largely affects mitochondrial integrity and induces the apoptotic pathway activation.

Next we decided to determine if cell death induction was associated to the release of iron from the iron-sulfur clusters in the mitochondrial matrix. In order to shed light on this event we tested whether the addition of an iron chelator could prevent this process. The iron chelator selected was deferiprone (DEF) previously reported to act specifically in the mitochondrial cell compartment and shown to be more specific with respect to other chelators in counteracting the iron-induced changes in mitochondria.[42] Lipid peroxidation, monitored as MDA production, in addition to thiol oxidation, measured as decrease of total thiol concentration, were evaluated in cells treated with Sel with or without preincubation with the iron chelator. DEF was able to partially

View Article Online
DOI: 10.1039/C9MT00090A

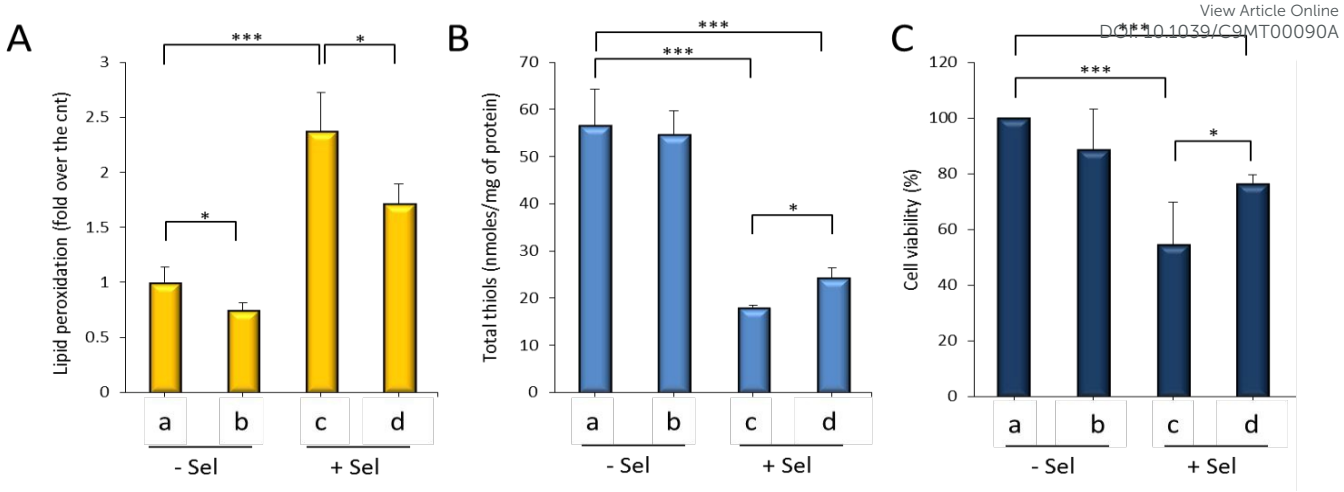

Figure 6. Effects of mitochondrial iron chelation on lipid and protein oxidation induced by Sel on HeLa cells. Hela cells were treated for 18 h with 15 µM Sel with (**b; d**) or without **(a; c**) pretreatment with the iron chelator (0.1 mM DEF) for 6 h. (**A**) Determination of lipid peroxidation in HeLa cells by means of the MDA assay as described in Experimental section. The graph reports the differences in lipid peroxidation shown as fold over the control. (**B**) Measurement of total thiols in HeLa cells. Total thiols are expressed as nmoles per mg of protein. (**C**) Cell viability assessed in HeLa cells utilizing the MTT test. The percentage of cell viability with respect to the control is reported. For each experiment the mean ± SD of three replicates is shown. (**a):** Cnt; (**b):** 0.1 mM DEF; (**c):** 15 µM Sel; (**d):** 0.1 mM DEF + 15 µM Sel. (*p<0.05; **p<0.01; ***p<0.001)

prevent the effect of Sel treatment on both lipid and total thiol oxidation (Fig. 6 A and B). Interestingly, deferoxamine which is another cell permeable iron chelator but lacking mitochondriotropic properties was completely ineffective (data not shown). This result further supports the idea of a role of iron-sulfur cluster release into mitochondria for the subsequent induction of cell death. Finally, in accordance to our hypothesis of a direct involvement of iron released from iron-sulfur clusters on apoptosis induction, we observed that treatment of HeLa cells with DEF prior to Sel addition, was able to increase cell viability with respect to the cells incubated with Sel alone, suggesting that cell death pathway activation is partially prevented (Fig. 6 C). Ferroptosis process has been investigated in the frame of Sel induced cell death. This process involves lipid peroxidation, glutathione depletion and down-regulation of glutathione peroxidase 4 (GPx4).[43] The latter, located both in the inner surface of the plasma membrane and in mitochondria, is devoted to removal of lipid hydroperoxides. Also other oxidizing agents, such as *tert*-butyl hydroperoxide, induced cell death in PC12 cells via ferroptosis, by decreasing GPx4 levels.[43] As reported in Fig. S 7 of the electronic supplementary information, a similar observation is apparent in our experimental conditions, suggesting a potential involvement of ferroptosis.

Discussion

The interaction of Sel with thiols leads to a shift toward oxidized conditions of sulfur residues, further accompanied by an autoxidation process resulting in ROS formation. Reactivity of Sel with thiol groups has been a research subject largely explored since a long time. Sel can react both with low molecular weight thiols such as GSH and protein thiols.[44-46] In particular, the reaction with glutathione is known in detail and, according to the conditions, can give rise to GSSG, GS-Se-SG, and H_2Se in addition to red metallic selenium (Se^0).[45] All this has significant consequences on cell viability and can be exploited in cancer thBindolierapy considering Sel as a potential therapeutic agent. Of note, when administered to cells, Sel shows a biphasic action as at low concentrations stimulates viability, while at concentrations above the nutritional requirement leads to cell death.[47] Previous research has shown that treatment with moderate concentrations of Sel offers the potential of a chemotherapeutic action which is enhanced by the concomitant inhibition of TrxR [48, 49] an enzyme overexpressed in several cancer cell lines.[50-55] According to the concentration and in line with previous observations,[48] cell treatment with Sel leads to a decrease of total thiols and to a depletion of glutathione indicating that the latter might be either covalently bound to proteins or lost from cells. Furthermore, Sel acts as a substrate of thiol dependent redox enzymes and is efficiently metabolized by TrxR1 and TrxR2.[56, 57] Similarly to thioredoxin reductase, Sel is also reduced by both Grx1 and Grx2 in a process where reduced species of selenium undergo redox cycling with oxygen and generate ROS.[58] Interestingly, it has been also reported that Sel treatment leads to a significant increase in protein glutathionylation that alters cell and mitochondrial functions.[58] For instance, the mitochondrial enzyme superoxide dismutase 2 (SOD2) can undergo glutathionylation involving a single specific cysteine suggesting a potential regulatory role of this enzyme through the reversible formation of a mixed disulfide with glutathione.[59] Like SOD2 , also SOD1, undergo glutathionylation particularly upon oxidative stress resulting in a pronounced structural rearrangement leading to a destabilization of the dimeric

structure that dissociates into monomers, releases metals and aggregates after partial unfolding. This process is attenuated by Grx overexpression.[60]

Of note, a protective effect of Trx on SOD2 was detected[61] suggesting a redox connection between SOD and the thiol-dependent redox systems.

In the present paper we report that, upon oxidation of glutathione by Sel, the dimeric iron-sulfur enzyme Grx2, undergo monomerization with the concomitant release of its iron-sulfur cluster. As previously reported, Grx2 plays a specific role in regulating cellular iron and in directing iron-sulfur cluster biogenesis.[12, 62] In dopaminergic neurons Grx2 knock-down by siRNA results in the decrease of incorporation of iron into mitochondrial enzymes containing iron-sulfur clusters with a concomitant significant increase of labile iron pool levels in mitochondria. In contrast, a parallel decrease of cytosolic iron, as a compensatory mechanism was observed.[63]Thus, the increase of free iron ions does not derive uniquely from Grx2 iron-sulfur clusters but the disassembly of Grx2 dimer could be a signal to induce further cascades towards mitochondrial iron overload. In addition, iron-sulfur centers are quite sensitive to oxidative stress. For instance $O_2^{\cdot-}$ oxidizes and inactivates the mitochondrial enzyme aconitase with a concomitant release of iron and hydrogen peroxide[64] and possibly other iron-sulfur proteins.[40, 65, 66] The formed pool of labile iron might be responsible of the peroxidative events occurring in mitochondria and potentially able to lead to cell to death. In fact, free iron can be deleterious for cell functions as it promotes Fenton chemistry together with stimulation of lipid peroxidation[67] therefore altering mitochondrial membrane properties. For instance, peroxidation of cardiolipin, a specific phospholipid of the inner mitochondrial membrane leads to alterations causing cell death.[40, 68]

Of note, the mitochondrial thiol redox enzymes Prx3,[69] Grx2 [20] and GPx4 [70] show anti apoptotic effects possibly related to a protection of cardiolipin from lipid peroxidation during the initial phase of apoptosis [40] so indicating the relevance of mitochondria redox conditions and in particular of the GSH pool for preserving cell viability. As reported in Fig. 6 A, we found a sensible increase of lipoperoxidation after treatment with Sel (Fig. 6 A) and a corresponding protective effect elicited by specific iron chelators and antioxidants, concomitant to the activation of Grx2.

The recently described process of ferroptosis, a distinct form of cell death dependent on iron and lipid peroxidation [71] has generated an increased interest also for the potential medical and pharmacological implications as some drugs inhibit this process.[72] In ferroptosis the labile iron pool, responsible for lipid peroxidation derives from endosomal uptake, degradation of the iron-binding protein ferritin and heme catabolism.[73] In this process a specific protective role is played by GPx4.[73, 74] Indeed, GPx4 acts as a negative regulator of ferroptosis as confirmed by GPx4 knockout mice.[75] A relationship between mitochondria alterations and ferroptosis has been recently observed as the ferroptosis inhibitor ferrostatin 1 protects PC12 cells from mitochondrial dysfunctions.[43] Furthermore, inhibition of iron uptake by mitochondria and the consequent lipid peroxidation is a condition that prevents ferroptosis.[76] Finally, in neuronal cells it was shown that ferroptosis induced by erastin depends on transactivation of BID to mitochondria causing loss of membrane potential and decrease of ATP leading to a morphological and functional damage ending in mitochondrial fragmentation.[77] Therefore, as shown by our results, mitochondria subjected to redox stress are able to stimulate an increase of the labile iron pool in which Grx2 iron-sulfur cluster is involved. The increased iron concentration is responsible for the occurrence of lipid peroxidation that in turn promotes the release of Cyt c and caspase activation in a process inhibited by iron chelators and antioxidants.

Conclusions

In conclusion, we have here shown that Grx2 forms inactive holo dimers in the mitochondrial matrix via the coordination of [2Fe-2S] clusters (Fig. 7 A). Upon oxidative stress induction, such as that observed after Sel treatment, the protein-cluster complex can sense the redox imbalance and undergoes fast disassembly through oxidation and detachment of the two glutathione molecules that normally stabilize the dimer (Fig. 7 B). Interestingly, a concomitant inhibition of both the thioredoxin and the glutathione systems seems to be necessary for the induction of protein monomerization. The monomeric Grx2 is active as a disulfide reductase, while the iron-sulfur cluster released, by increasing the amount of free iron ions in mitochondria, can induce lipid peroxidation and, eventually, a drop of the mitochondrial membrane potential and cell death (Fig. 7 C). The fact that a mitochondriotropic iron chelator can block the lipid and protein oxidation and cell death suggests a new function of Grx2 as a regulatory protein for the induction of cell apoptosis upon oxidative imbalance in mitochondria and underlines the key function of Grx2-dependent mechanism of oxidative stress sensing in the mitochondrial signaling network.

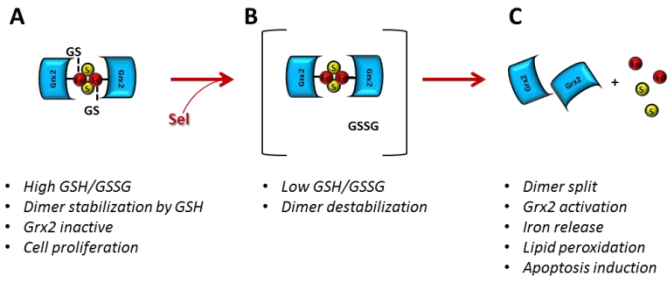

Figure 7. Sequence of events leading to Grx2 activation in mitochondria following oxidative stress induction. In reducing conditions, mitochondrial Grx2 binds a [2Fe-2S] cluster with its active site forming a dimer stabilized by two molecules of glutathione (**A**). When the redox homeostasis is lost and the ratio between reduced and oxidized glutathione decreases, as in the case of Sel administration, the two molecules of GSH are oxidized, they detach from the cluster and lead to the destabilization of the Grx2 dimer (**B**). At this point the dimer splits, Grx2 gets activated, and the increased iron level in mitochondria triggers lipid peroxidation and induction of

the apoptotic pathway (**C**). Red circles: Fe atoms, Yellow circles: S atoms.

Conflicts of interest

There are no conflicts to declare.

Abbreviations

AIS, 4-acetamido-4'-((iodoacetyl) amino) stilbene-2,2'-disulfonic acid; AF, auranofin; BHT, butylated hydroxytoluene; BSO, buthionine sulfoximine; Cyt c, cytochrome c; DEF, deferiprone, 3-hydroxy-1,2-dimethyl-4(1H)-pyridone; ΔΨm, mitochondrial membrane potential; DTNB, 5,5'-dithiobis(2-nitrobenzoic acid); [2Fe-2S], iron-sulfur cluster; GPx4, glutathione peroxidase 4; Grx1, glutaredoxin 1; Grx2, glutaredoxin 2; Grx5, glutaredoxin 5; GSH, reduced glutathione; GSSG, oxidized glutathione; HEDS, hydroxyethyl disulfide; H2O2, hydrogen peroxide; MDA, malondialdehyde; MTT, 3-[4,5-dimethylthiazol-2-yl]-2,5-diphenyltetrazolium bromide; PBS, phosphate buffer saline; PTA, phosphotungstic acid; ROS, reactive oxygen species; Sel, sodium selenite; TMRM, tetramethylrhodamine methyl ester; Trx1, thioredoxin 1; Trx2, thioredoxin 2; TrxR1, thioredoxin reductase 1; TrxR2, thioredoxin reductase 2.

Acknowledgements

Authors acknowledge Prof. Valentina Gandin of the Dept. of Pharmacological Sciences at the University of Padova for her help with the atomic absorption facility, Prof. Aristi Fernandes of the Karolinska Institutet in Stockholm, for kindly providing the human recombinant Grx2 and Prof Tito Calì of the Dept. of Biomedical Sciences at the University of Padova for the critical reading of the manuscript. M.P.R. and V.S. acknowledge BIRD187299/18 granted by University of Padova (Italy).

References

1. C.H. Lillig and A. Holmgren, *Antioxid Redox Signal*, 2007, **9**, 25-47.
2. E.S. Arner, *Biochim Biophys Acta*, 2009, **1790**, 495-526.
3. A. Bindoli and M.P. Rigobello, *Antioxid Redox Signal*, 2013, **18**, 1557-93.
4. A. Holmgren, *J Biol Chem*, 1989, **264**, 13963-66.
5. A.P. Fernandes and A. Holmgren, *Antioxid Redox Signal*, 2004, **6**, 63-74.
6. A. Holmgren, *Annu Rev Biochem*, 1985, **54**, 237-71.
7. H. Ye, S.Y. Jeong, M.C. Ghosh, G. Kovtunovych, L. Silvestri, D. Ortillo, N. Uchida, J. Tisdale, C. Camaschella, and T.A. Rouault, *J Clin Invest*, 2010, **120**, 1749-61.
8. C.H. Lillig, M.E. Lonn, M. Enoksson, A.P. Fernandes, and A. Holmgren, *Proc Natl Acad Sci U S A*, 2004, **101**, 13227-32.
9. M. Lundberg, A.P. Fernandes, S. Kumar, and A. Holmgren, *Biochem Biophys Res Commun*, 2004, **319**, 801-09.
10. C. Johansson, C.H. Lillig, and A. Holmgren, *J Biol Chem*, 2004, **279**, 7537-43.
11. C.H. Lillig, C. Berndt, O. Vergnolle, M.E. Lonn, C. Hudemann, E. Bill, and A. Holmgren, *Proc Natl Acad Sci U S A*, 2005, **102**, 8168-73.
12. C. Berndt, C. Hudemann, E.M. Hanschmann, R. Axelsson, A. Holmgren, and C.H. Lillig, *Antioxid Redox Signal*, 2007, **9**, 151-57.
13. E.M. Hanschmann, J.R. Godoy, C. Berndt, C. Hudemann, and C.H. Lillig, *Antioxid Redox Signal*, 2013, **19**, 1539-605.
14. E.A.S. Liedhegner, X.H. Gao, and J.J. Mieyal, *Antioxid Redox Signal*, 2012, **16**, 543-66.
15. S.M. Beer, E.R. Taylor, S.E. Brown, C.C. Dahm, N.J. Costa, M.J. Runswick, and M.P. Murphy, *J Biol Chem*, 2004, **279**, 47939-51.
16. R.J. Mailloux, S.L. McBride, and M.E. Harper, *Trends Biochem Sci*, 2013, **38**, 592-602.
17. Y. Ouyang, Y. Peng, J. Li, A. Holmgren, and J. Lu, *Metallomics*, 2018, **10**, 218-28.
18. C. Berndt and C.H. Lillig, *Antioxid Redox Signal*, 2017, **27**, 1235-51.
19. G.N. Kanaan, B. Ichim, L. Gharibeh, W. Maharsy, D.A. Patten, J.Y. Xuan, A. Reunov, P. Marshall, J. Veinot, K. Menzies, M. Nemer, and M.E. Harper, *Redox Biol*, 2018, **14**, 509-21.
20. M. Enoksson, A.P. Fernandes, S. Prast, C.H. Lillig, A. Holmgren, and S. Orrenius, *Biochem Biophys Res Commun*, 2005, **327**, 774-79.
21. C. Johansson, K.L. Kavanagh, O. Gileadi, and U. Oppermann, *J Biol Chem*, 2007, **282**, 3077-82.
22. G.L. Ellman, *Arch Biochem Biophys*, 1959, **82**, 70-77.
23. F. Tietze, *Anal Biochem*, 1969, **27**, 502-22.
24. M.E. Anderson, *Methods Enzymol*, 1985, **113**, 548-55.
25. O.H. Lowry, N.J. Rosebrough, A.L. Farr, and R.J. Randall, *J Biol Chem*, 1951, **193**, 265-75.
26. D.A. Clayton and G.S. Shadel, *Cold Spring Harb Protoc*, 2014, **2014**, pdb top074542.
27. J.J. Mieyal, D.W. Starke, S.A. Gravina, C. Dothey, and J.S. Chung, *Biochemistry*, 1991, **30**, 6088-97.
28. N. Raghavachari and M.F. Lou, *Exp Eye Res*, 1996, **63**, 433-41.
29. D.K. Myers and E.C. Slater, *Biochem J*, 1957, **67**, 558-72.
30. M.M. Bradford, *Anal Biochem*, 1976, **72**, 248-54.
31. X.H. Gao, S. Qanungo, H.V. Pai, D.W. Starke, K.M. Steller, H. Fujioka, E.J. Lesnefsky, J. Kerner, M.G. Rosca, C.L. Hoppel, and J.J. Mieyal, *Redox Biol*, 2013, **1**, 586-98.
32. B.A. Stanley, V. Sivakumaran, S. Shi, I. McDonald, D. Lloyd, W.H. Watson, M.A. Aon, and N. Paolocci, *J Biol Chem*, 2011, **286**, 33669-77.
33. V. Scalcon, M. Salmain, A. Folda, S. Top, P. Pigeon, H.Z.S. Lee, G. Jaouen, A. Bindoli, A. Vessieres, and M.P. Rigobello, *Metallomics*, 2017, **9**, 949-59.
34. C.C. Tsen and H.B. Collier, *Can J Biochem Physiol*, 1960, **38**, 981-87.
35. I. Anundi, A. Stahl, and J. Hogberg, *Chem Biol Interact*, 1984, **50**, 277-88.
36. J. Tamarit, G. Belli, E. Cabiscol, E. Herrero, and J. Ros, *J Biol Chem*, 2003, **278**, 25745-51.
37. H.V. Pai, D.W. Starke, E.J. Lesnefsky, C.L. Hoppel, and J.J. Mieyal, *Antioxid Redox Signal*, 2007, **9**, 2027-33.
38. M.M. Gallogly, D.W. Starke, A.K. Leonberg, S.M. Ospina, and J.J. Mieyal, *Biochemistry*, 2008, **47**, 11144-57.
39. A. Bindoli, *Free Radic Biol Med*, 1988, **5**, 247-61.

40. S. Orrenius, V. Gogvadze, and B. Zhivotovsky, *Annu Rev Pharmacol Toxicol*, 2007, **47**, 143-83.
41. J. Montero, M. Mari, A. Colell, A. Morales, G. Basanez, C. Garcia-Ruiz, and J.C. Fernandez-Checa, *Bba-Bioenergetics*, 2010, **1797**, 1217-24.
42. H. Glickstein, R.B. El, G. Link, W. Breuer, A.M. Konijn, C. Hershko, H. Nick, and Z.I. Cabantchik, *Blood*, 2006, **108**, 3195-203.
43. C.H. Wu, W.W. Zhao, J. Yu, S.J. Li, L.G. Lin, and X.P. Chen, *Sci Rep*, 2018, **8**, 574.
44. E.P. Painter, *Chem. Rev.*, 1941, **28**, 179–213.
45. H.E. Ganther, *Biochemistry*, 1971, **10**, 4089-98.
46. H.E. Ganther and C. Corcoran, *Biochemistry*, 1969, **8**, 2557-63.
47. A.P. Fernandes and V. Gandin, *Bba-Gen Subjects*, 2015, **1850**, 1642-60.
48. M.P. Rigobello, V. Gandin, A. Folda, A.K. Rundlof, A.P. Fernandes, A. Bindoli, C. Marzano, and M. Bjornstedt, *Free Radic Biol Med*, 2009, **47**, 710-21.
49. M. Selenius, A.P. Fernandes, O. Brodin, M. Bjornstedt, and A.K. Rundlof, *Biochem Pharmacol*, 2008, **75**, 2092-99.
50. C. Cadenas, D. Franckenstein, M. Schmidt, M. Gehrmann, M. Hermes, B. Geppert, W. Schormann, L.J. Maccoux, M. Schug, A. Schumann, C. Wilhelm, E. Freis, K. Ickstadt, J. Rahnenfuhrer, J.I. Baumbach, A. Sickmann, and J.G. Hengstler, *Breast Cancer Res*, 2010, **12**, R44.
51. D.T. Lincoln, F. Al-Yatama, F.M. Mohammed, A.G. Al-Banaw, M. Al-Bader, M. Burge, F. Sinowatz, and P.K. Singal, *Anticancer Res*, 2010, **30**, 767-75.
52. S.S. Singh, Y. Li, O.H. Ford, C.S. Wrzosek, D.C. Mehedint, M.A. Titus, and J.L. Mohler, *Transl Oncol*, 2008, **1**, 153-57.
53. K. Kahlos, Y. Soini, M. Saily, P. Koistinen, S. Kakko, P. Paakko, A. Holmgren, and V.L. Kinnula, *Int J Cancer*, 2001, **95**, 198-204.
54. D.T. Lincoln, E.M. Ali Emadi, K.F. Tonissen, and F.M. Clarke, *Anticancer Res*, 2003, **23**, 2425-33.
55. J.H. Choi, T.N. Kim, S. Kim, S.H. Baek, J.H. Kim, S.R. Lee, and J.R. Kim, *Anticancer Res*, 2002, **22**, 3331-35.
56. S. Kumar, M. Bjornstedt, and A. Holmgren, *Eur J Biochem*, 1992, **207**, 435-39.
57. M.P. Rigobello, A. Folda, A. Citta, G. Scutari, V. Gandin, A.P. Fernandes, A.K. Rundlof, C. Marzano, M. Bjornstedt, and A. Bindoli, *Free Radic Biol Med*, 2011, **50**, 1620-29.
58. M. Wallenberg, E. Olm, C. Hebert, M. Bjornstedt, and A.P. Fernandes, *Biochem J*, 2010, **429**, 85-93.
59. I. Castellano, F. Cecere, A. De Vendittis, R. Cotugno, A. Chambery, A. Di Maro, A. Michniewicz, G. Parlato, M. Masullo, E.V. Avvedimento, E. De Vendittis, and M.R. Ruocco, *Biopolymers*, 2009, **91**, 1215-26.
60. R.L. Redler, K.C. Wilcox, E.A. Proctor, L. Fee, M. Caplow, and N.V. Dokholyan, *Biochemistry*, 2011, **50**, 7057-66.
61. F. Cecere, A. Iuliano, F. Albano, C. Zappelli, I. Castellano, P. Grimaldi, M. Masullo, E. De Vendittis, and M.R. Ruocco, *J Biomed Biotechnol*, 2010, **2010**, 801726.
62. J. Couturier, J. Przybyla-Toscano, T. Roret, C. Didierjean, and N. Rouhier, *Bba-Mol Cell Res*, 2015, **1853**, 1513-27.
63. D.W. Lee, D. Kaur, S.J. Chinta, S. Rajagopalan, and J.K. Andersen, *Antioxid Redox Signal*, 2009, **11**, 2083-94.
64. I. Fridovich, *J Biol Chem*, 1997, **272**, 18515-17.
65. E. Cadenas and K.J.A. Davies, *Free Radic Biol Med*, 2000, **29**, 222-30.
66. Y. Zhang, O. Marcillat, C. Giulivi, L. Ernster, and K.J. Davies, *J Biol Chem*, 1990, **265**, 16330-36. DOI: 10.1039/C9MT00090A
67. B. Halliwell and J.M.C. Gutteridge, Fifth edition. ed. 2015, Oxford, United Kingdom: Oxford University Press. 905 pages.
68. V.E. Kagan, V.A. Tyurin, J.F. Jiang, Y.Y. Tyurina, V.B. Ritov, A.A. Amoscato, A.N. Osipov, N.A. Belikova, A.A. Kapralov, V. Kini, I.I. Vlasova, Q. Zhao, M.M. Zou, P. Di, D.A. Svistunenko, I.V. Kurnikov, and G.G. Borisenko, *Nat Chem Biol*, 2005, **1**, 223-32.
69. T.S. Chang, C.S. Cho, S. Park, S. Yu, S.W. Kang, and S.G. Rhee, *J Biol Chem*, 2004, **279**, 41975-84.
70. K. Nomura, H. Imai, T. Koumura, T. Kobayashi, and Y. Nakagawa, *Biochem J*, 2000, **351**, 183-93.
71. S.J. Dixon, K.M. Lemberg, M.R. Lamprecht, R. Skouta, E.M. Zaitsev, C.E. Gleason, D.N. Patel, A.J. Bauer, A.M. Cantley, W.S. Yang, B. Morrison, 3rd, and B.R. Stockwell, *Cell*, 2012, **149**, 1060-72.
72. T.M. Seibt, B. Proneth, and M. Conrad, *Free Radic Biol Med*, 2019, **133**, 144-52.
73. M. Maiorino, M. Conrad, and F. Ursini, *Antioxid Redox Signal*, 2018, **29**, 61-74.
74. F. Ursini, M. Maiorino, M. Valente, L. Ferri, and C. Gregolin, *Biochim Biophys Acta*, 1982, **710**, 197-211.
75. Y. Xie, W. Hou, X. Song, Y. Yu, J. Huang, X. Sun, R. Kang, and D. Tang, *Cell Death Differ*, 2016, **23**, 369-79.
76. H. Yuan, X.M. Li, X.Y. Zhang, R. Kang, and D.L. Tang, *Biochem Biophys Res Commun*, 2016, **478**, 838-44.
77. S. Neitemeier, A. Jelinek, V. Laino, L. Hoffmann, I. Eisenbach, R. Eying, G.K. Ganjam, A.M. Dolga, S. Oppermann, and C. Culmsee, *Redox Biol*, 2017, **12**, 558-70.